Nonlinear Prediction of Aerodynamic Loads on Lifting Surfaces

O. A. Kandil,* D. T. Mook,† and A. H. Nayfeh‡
Virginia Polytechnic Institute and State University, Blacksburg, Va.

A numerical method is developed to predict the distributed and total aerodynamic loads on nonplanar lifting surfaces for steady, inviscid, incompressible flow. There are no restrictions on aspect ratio, planform, camber, or angle of attack as long as separation occurs along the sharp edges only. The lifting surface is represented by a lattice of discrete vortex lines. The wakes generated by leading-edge, tip, and training-edge separation are represented by families of discrete, nonintersecting vortex lines; each line is composed of a series of straight, finite segments and one straight, semi-infinite segment; the positions of these lines are obtained as part of the solution. Rectangular, arrowhead, and delta wings are considered in the numerical examples. The predicted results agree closely with experimental data.

Nomenclature

$\mathcal{R}$	= aspect ratio
$2b$	= dimensionless wing span
c_r	= dimensionless root chord
c_{m_z}	= pitching-moment coefficient (about the z-axis)
c_n	= normal-force coefficient
$c'_{n_{loc}}$	= local-normal-force coefficient
c_p	= pressure coefficient
CP_z	= center of pressure measured from the z-axis
x,y,z	= Cartesian coordinate system
α	= angle of attack
β	= sweep-back angle

I. Introduction

WINGS designed for supersonic flight are often highly swept and thin and have sharp leading edges and/or tips. When operating subsonically, these wings are often at high angles of attack. Consequently, the prediction of the total aerodynamic loads and the load distributions in the subsonic regime is complicated by the need to account for leading-edge and tip separation. Considering these predictions to be a primary goal, we developed a general numerical scheme which is applicable to all aspect ratios, planforms, cambers, and angles of attack as long as separation occurs along the sharp edges only.

In the present paper, we describe the flowfield of primary interest and some of the earlier attempts to model it, then we describe the present method, and finally we present comparisons of the present predicted results with other predicted results and experimental data.

II. Description of Flowfield

For highly swept delta wings, at least three distinct cores and lines of separation have been observed in the flowfields produced by leading-edge separation. In addition to the primary vortex and the line of separation at the leading edge, Marsden, Simpson, and Rainbird,[1] Peckham,[2] Bergesen and Porter,[3] and Hummel[4] observed a secondary vortex core and line of separation behind the leading edge. The direction of the vorticity in this secondary vortex is opposite that in the primary vortex. The secondary vortex is located above the wing, but below the primary vortex, and inboard from the leading edge. Considering the relative sizes of the primary and secondary vortices downstream from the trailing edge, Bergesen and Porter suspected that the secondary vortex may significantly influence the flowfield. However, Peckham found that the strength of the secondary vortex is only about 5% of the strength of the primary vortex. In addition, Hummel found that, in the region between the secondary line of separation and the leading edge, it is sometimes possible to observe a tertiary vortex and line of separation. The direction of the vorticity in the tertiary vortex is the same as that in the primary vortex. The tertiary vortex is relatively very small. A schematic drawing of these three vortex regions is presented in Fig. 1. A similar flowfield may exist near the wing tip, though the experiments of Winter,[5] Scholz,[6] Ermolenko,[7] Belotserkovskiy,[8] and Lamar[9] apparently were concerned with determining the aerodynamic coefficients of the various wings, not with the structure of the tip vortex systems.

The strong crossflow produced by the leading-edge and tip vortex systems is responsible for these low-aspect wings having the desirable feature of generating large lift at large angles of attack. It appears that vortex bursting or breakdown is the phenomenon which accompanies the reduction in lift as the angle continues to increase. Vortex bursting was observed by Hummel[4] for a delta wing of unit aspect ratio and by

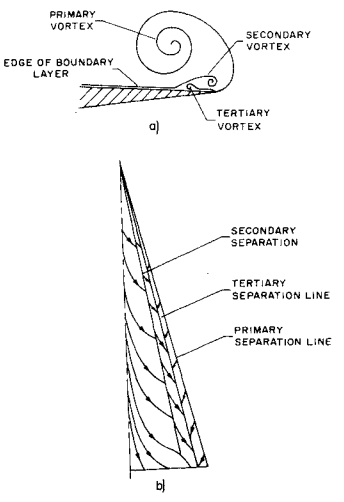

Fig. 1 Types of separation near leading edge of delta wing: a) section normal to the leading edge, b) lines of separation.

Presented as AIAA Paper 74-503 at the AIAA 7th Fluid and Plasma Dynamics Conference, Palo Alto, California, June 17-19, 1974; submitted July 17, 1974; revision received April 11, 1975. This work was supported by the NASA Langley Research Center under Grant NGR 47-004-090. The many helpful comments and discussions of E.C. Yates are greatly appreciated.

Index category: Aircraft Aerodynamics (including Component Aerodynamics).

*Assistant Professor, Engineering Science and Mechanics Department. Member AIAA.

†Associate Professor, Engineering Science and Mechanics Department. Member AIAA.

‡Professor, Engineering Science and Mechanics Department. Member AIAA.

Wentz and Kohlman[10] for various other planforms and aspect ratios.

The feasibility of accounting for leading-edge and tip separation before vortex bursting occurs with an inviscid model was established in at least two experiments: Winter[5] in considering rectangular plates varied the Reynolds number over the approximate range $0.3\text{-}1.7\times10^6$, while Peckham[2] in considering delta wings varied the Reynolds number over the approximate range $2\text{-}8\times10^6$. Both observed that the aerodynamic characteristics are practically independent of the Reynolds number. Consequently, it appears that one may consider the flowfield to be governed by Laplace's equation. However, the lifting-surface models usually used for small angles of attack, including vortex-lattice methods employing horseshoe elements, cannot be expected to treat these flows satisfactorily, unless some modifications are made so that they can accurately predict the influence of the leading-edge and tip vortex systems.

The effect of thickness was investigated by Peckham[2] and Belotserkovskiy;[8] both found significant decreases in the aerodynamic coefficients when the thickness was increased. The maximum thicknesses considered were 12% by Peckham and 30% by Belotserkovskiy.

The effect of the subsonic freestream Mach number on the aerodynamic coefficients was studied by a number of investigators, including Sutton,[11] Squire, Jones, and Stanbrook,[12] Bateman and Haines,[13] Dee and Nicholas,[14] and Stahl, Hartmann and Schneider.[15] They found that the load coefficients increase slightly as the freestream Mach number increases.

The effect of the leading-edge camber on the aerodynamic characteristics of slender delta wings was also investigated. Wentz[16] found that the leading-edge camber (conical or apex camber) has a slight effect on the total lift, but it reduces the drag due to lift at high angles of attack. Apex camber produces higher pitching-moment coefficients than conical camber or no camber.

III. Earlier Attempts to Model Flowfield

A. Analytical Attempts

A number of analytical attempts to model the flowfield were made.[17-28] The basic shortcoming of the unsuccessful attempts stems from the inadequate manner in which the wakes adjoining the sharp edges were modeled; for delta wings; slender-body and conical-flow assumptions were often used (the observations of Earnshaw[29] seem to discredit these assumptions). One successful technique for predicting the lift, due to Polhamus, is based on the leading-edge suction analogy,[26-28] however, this method does not have the capability of predicting distributed loads.

B. Numerical Attempts

Generally, the numerical methods have used a vortex lattice to represent the lifting surface and nonintersecting discrete vortex lines to represent the wakes. These methods can be divided into two categories—linear and nonlinear methods.

1. Linear Methods

With the linear methods,[30-35] the so-called horseshoe elements are used to form the lattice as well as the lines modeling the wake adjoining the trailing edge. The direction of these lines is prescribed, not obtained as part of the solution, and no attempt is made to model the tip or leading-edge vortex systems. Consequently, the only unknowns are the circulations of the horseshoe elements. These are found from the no-penetration boundary condition and, consequently, the entire problem is linear. These methods yield accurate results for small angles of attack only; thus, they are of very limited usefulness for the small-aspect wings given priority here.

2. Nonlinear Methods

To extend the range of applicability of the discrete-vortex methods, efforts were made to include models of the tip or leading-edge vortex systems. The first attempt to model the tip vortex system was made by Ermolenko,[7] who considered rectangular, small-aspect wings. He modeled the wing surface with a series of spanwise vortex lines instead of a lattice and, consequently, he ignored the wake adjoining the trailing edge. At the wing tips, he joined these lines to other straight lines, which lay in planes perpendicular to the wing surface. Then, through iteration, he simultaneously aligned each line in the tip vortex systems with the projection of the velocity onto the perpendicular planes at the points where the spanwise lines intersect the tips and satisfied the no-penetration condition at the midpoint of each spanwise strip.

Belotserkovskiy[8] greatly improved Ermolenko's model by using a lattice to represent the lifting surface and making each line in the wakes adjoining the tip and trailing edge consist of a finite number of finite segments and one semi-infinite segment. Then, through iteration, he simultaneously aligned each finite segment in the wake with the velocity at its midpoint and satisfied the no-penetration boundary condition.

Following Belotserkovskiy, Mook and Maddox[36] devised a model for the leading-edge vortex system on highly swept delta wings. This model was superimposed on a horseshoe lattice representing the lifting surface and the trailing-edge vortex system. Rehbach[37,38] first developed a method to treat rectangular and arrowhead planforms and then extended the method to delta wings. We present here a general method which is applicable to any planform, camber, or angle of attack, as long as separation occurs along the sharp edges only. Both Rehbach's and the present method are an improvement over the method of Mook and Maddox because neither prescribes the position of the trailing-edge wake and both are better suited to handle large camber. The present method appears to be quite similar to Rehbach's for rectangular and arrowhead wings, but the ways in which the extensions to delta wings were effected are quite different. The salient difference is discussed later.

IV. Description of Basic Method

The steady flow of an incompressible fluid past a thin wing can be simulated by a bound-vortex sheet representing the lifting surface and free-vortex sheets representing the wakes adjoining the sharp edges where separation occurs.

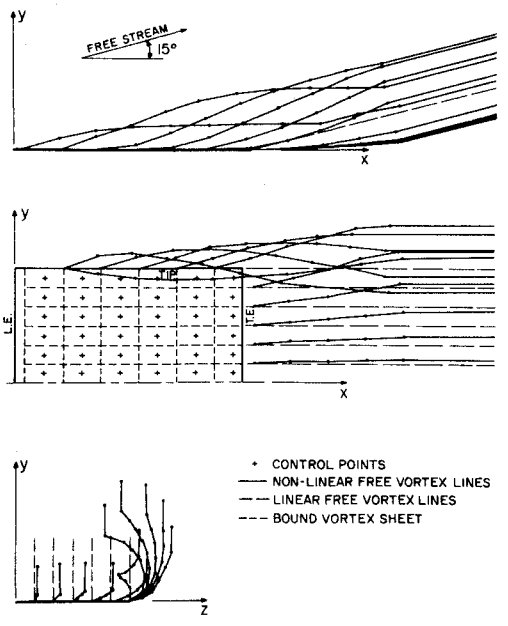

Fig. 2 Positions of free-vortex lines for rectangular wing, $\mathcal{A}=1$, 6×6 lattice.

The bound sheet is represented by a lattice and the free sheets by a series of nonintersecting lines. The points of intersection on the lattice are joined by straight vortex segments, and each vortex line representing the free vortex sheet is composed of a series of short, straight segments, except the last segment, which is semi-infinite and extends downstream. The directions of the short segments in the wakes are determined as part of the solution, but the last segment is parallel to the freestream. (The arrangements for parallelogram and delta wings are shown in Figs. 2 and 3.)

The lattice divides the lifting surface into elements which are generally nonplanar. Associated with each element is a control point, denoted by +, where the normal component of velocity is forced to vanish; a spanwise vortex segment along its forward edge; and a chordwise vortex segment along its outboard edge. The actual surface of an element is approximated by its projection onto the plane which is perpendicular to the vector product of the diagonals and contains the centroid of the four corners. The velocity generated by the vortex segements is determined by using the Biot-Savart law. The force on a bound-vortex segment is calculated by applying the Kutta-Joukowski theorem at its midpoint (see the details of the velocity and force calculation in Ref. 41).

When using discrete vortex lines, one satisfies the Kutta condition by not placing any vortex segments between the control points of the last row of elements and the trailing edge and the control points of the last elements in each row and the wing tip (leading edge) in the case of a parallelogram wing (delta wing) and by making the vortex segments be perpendicular to the edge. Here, it is assumed that the edges where the Kutta condition is imposed are sharp, so that one knows where the wakes are attached.

The basic unknowns of the problem are the circulations and the directions of the free-vortex segments. These unknowns are determined by simultaneously requiring: a) the normal component of the velocity to vanish at each control point of the bound-vortex lattice, b) the circulation to be spatially conserved at each intersection of the lattice, and c) each segment, except the last in each line of the wake to be force free. The solution is obtained by the following procedure. Initial directions are assigned to each segment in the entire wake. The initial configuration may conform to that which is used in the so-called linear analysis, or it may conform to a previously obtained solution for a nearby angle of attack. With the position of the wake specified the circulation distribution is determined by satisfying requirements a) and b). Then, with the circulation distribution fixed, each finite segment in the wakes is aligned with the velocity at its upstream end. Because the velocity field changes when the positions of the segments change, an iterative procedure is employed to effect this step. After each iteration, the magnitude of the displacement of each downstream end is calculated. Convergence is achieved when the maximum of these magnitudes is less than a prescribed value.

At this point, the vortex lines in the wake are aligned with the streamlines of the flow, but because the configuration of the wake was changed, the no-penetration condition is no longer satisfied. Consequently, with the wake fixed in its new position, the circulation distribution is redetermined. Then, with the new circulation distribution fixed, the vortex lines in the wakes are again aligned with the streamlines. This procedure is repeated until the maximum of the magnitudes of the displacements of the downstream ends of the finite segments for two successive circulation distributions is less than a prescribed value.

For a given wing and angle of attack, we consider convergence to be achieved if a) for a fixed number of rows and columns of the bound-vortex lattice the shape of the wake converges, as just described, and b) the predicted aerodynamic loads converge as the number of rows and columns increases. After the forces acting on the spanwise and chordwise segments of the lattice are calculated, the aerodynamic parameters, such as the normal-force and pitching-moment coefficients, can be easily obtained. The average pressure coefficient over an elemental area is found by dividing the sum of one-half the normal forces acting on the vortex segements bounding this element by its area. An exception is the leading row of elements; the entire force on the forward spanwise segment is used.

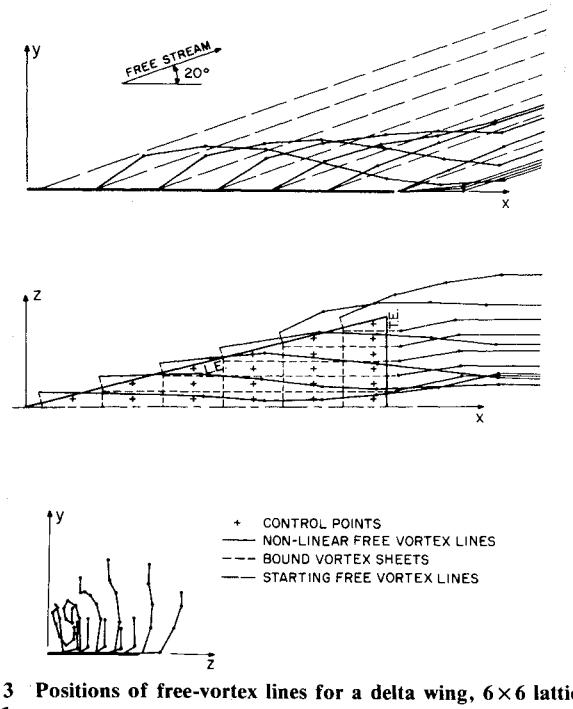

Fig. 3 Positions of free-vortex lines for a delta wing, 6×6 lattice, $\mathcal{R}=1$.

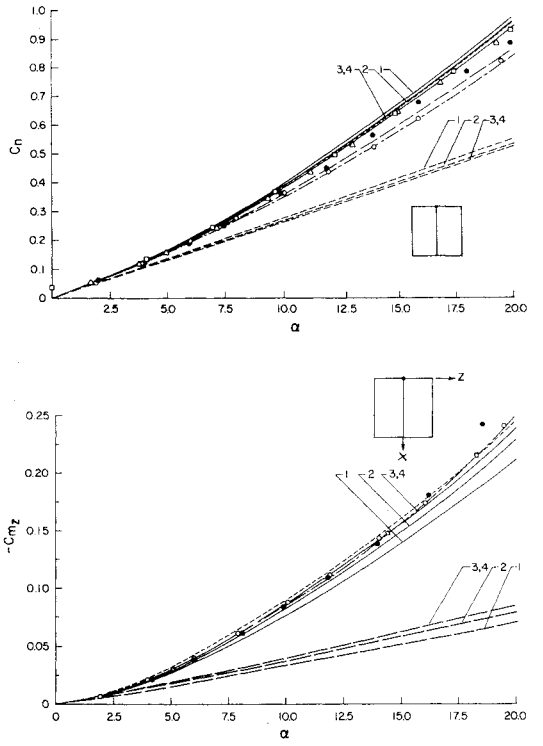

Fig. 4 Normal-force and pitching-moment coefficients vs angle of attack, $\mathcal{R}=1$. Numerical results: ------ Belotserkovskiy;[8] —·— Ermolenko;[7] —— Bradley, et al.[28] ——— Linear, —— Nonlinear: Present method. Curve No. 1:4×4 lattice; curve No. 2:6×6 lattice; curve No. 3: 9×7 lattice; curve No. 4; 9×9 lattice. Experimental Results: • Belotserkovskiy;[8] ○ Ermolenko;[7] □ Winter;[6] △ Scholz.[6]

V. Numerical Examples

This procedure was used to determine the distributed and total loads on some thin, flat wings having rectangular, swept-back, and delta planforms. For the rectangular and swept-back (with parallel leading and trailing edges) wings, we consider the leading edges to be rounded and the wing tips and trailing edges to be sharp. In the case of delta wings, we consider all the edges to be sharp. These wings have been the subject of earlier experimental, analytical, and numerical investigations and, consequently, they provide an excellent basis for evaluating the present method.

A. Rectangular and Swept-Back Wings

Figure 2 depicts an actual solution in which the positions of the finite segments in the wake were determined. The arrangement of the vortex lines is shown in three views. The dotted lines denote the bound-vortex lattice and the dashed lines show the initial position of the lines in the wake. This figure is similar to those obtained by Belotserkovskiy[8] and Rehbach.[37]

In Fig. 4a, the normal-force coefficient is given as a function of the angle of attack. Here, we illustrate the convergence of the method as the number of elements is increased. The curves based on the lattices having nine rows by seven columns and nine rows by nine columns are practically identical. This convergence was not shown by either Belotserkovskiy[8] or Rehbach.[37,38] If the discrete-vortex model is suitable, this test must be satisfied.

Apparently, the differences among the various sets of experimental data can be attributed to the manner in which the wing tip is beveled (see, e.g., Bartlett and Vidal,[39] Kirkpatrick,[40] and Kandil[41]). The smaller the bevel angle is, the farther inboard the cores of the wing-tip vortex systems are, the greater the crossflow is, and, consequently, the higher the lift is.

The "linear" results are based on the lattice in which the last chordwise vortex lines are attached to the wing tip and the vortex lines adjoining the trailing edge are straight and parallel to the freestream velocity.

In Fig. 4b, the pitching-moment coefficient is given as a function of the angle of attack. The good agreement between the predictions and the data is a result of the proper choice of the position of the wing with respect to the lattice; specifically, the spanwise-vortex lines are placed at one quarter of the chordwise dimension of the elements.

In Fig. 5, the normal-force and pitching-moment coefficients are given as functions of the aspect ratio for a fixed angle of attack. One expects the results obtained from the linear and nonlinear analyses to agree when the aspect ratio is large because wing-tip vortices significantly affect a smaller percentage of the lifting surface. For the present results the difference is less than 5% when the aspect ratio is 4½.

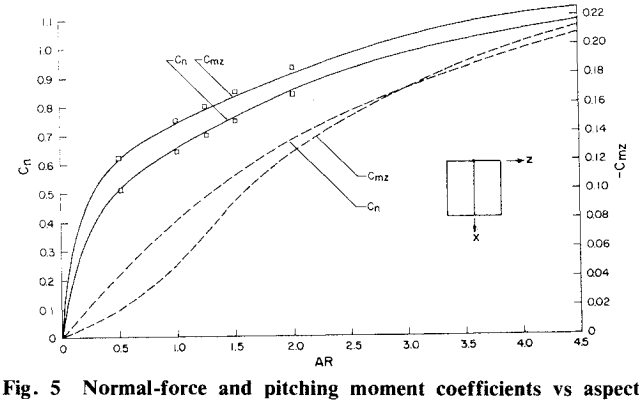

Fig. 5 Normal-force and pitching moment coefficients vs aspect ratio $\alpha = 15°$ Numerical Results: Present method (6×6 lattice):——— Linear; —— Nonlinear. Experimental Results: □ Winter.[5]

Figure 6 shows that the predicted spanwise variation of the local normal-force coefficient is in good agreement with the experimental results of Scholz. We note that the nonlinear analysis predicts higher loads than the linear analysis. In addition, the chordwise sections near the wing tip have higher loads than the other sections.

In Fig. 7, the spatial variation of the pressure coefficient is given. This figure shows the opposite trends predicted by the linear and nonlinear analyses.

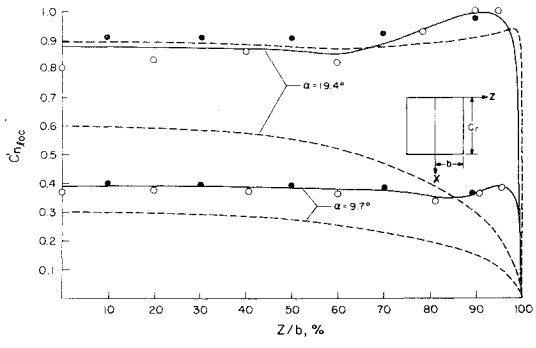

Fig. 6 Spanwise variation of local normal-force coefficient for different angles of attack, $\mathcal{R} = 1$. Numerical results: —— Gersten;[18] • Rehbach.[37] Present method (9×7 lattice): ——— Linear; —— Nonlinear. Experimental results: ○ Scholz.[6]

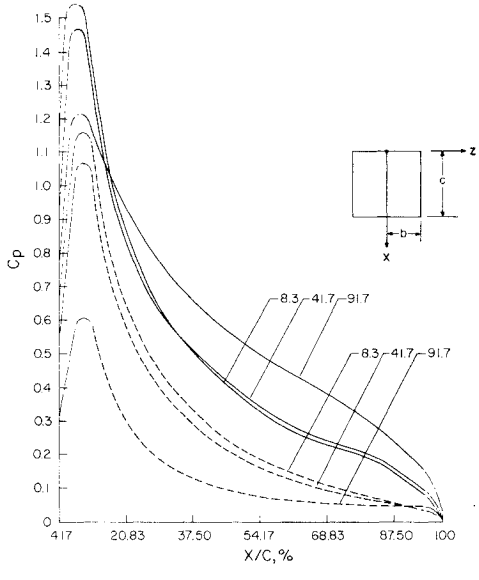

Fig. 7 Spatial variation of pressure coefficient. Each curve is for constant $(z/b) \times 100$, $\mathcal{R} = 1$, $\alpha = 15°$. 6×6 lattice: ——— Linear; —— Nonlinear; ——— Extrapolated.

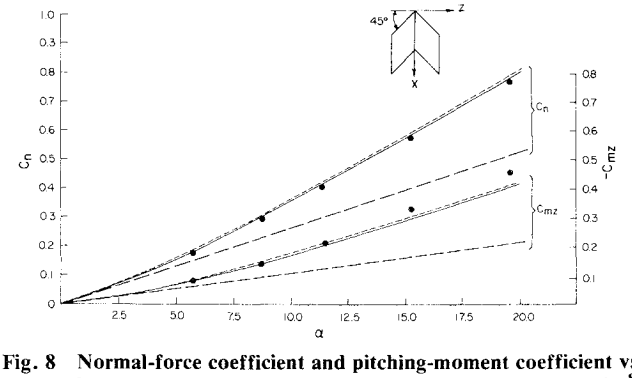

Fig. 8 Normal-force coefficient and pitching-moment coefficient vs angle of attack, $\mathcal{R} = 1$. Numerical Results: ------Belotserkovskiy;[8] Present method (7×5 lattice): ——— Linear; ——Nonlinear. Experimental Results: • Jacob [taken from Gersten[18]].

In Fig. 8, the normal-force and pitching-moment coefficients for a 45-deg swept-back wing are given as functions of the angle of attack. Comparing this figure with Fig. 4, one can see that for the same aspect ratio the rectangular wing has a higher normal-force coefficient and a lower pitching-moment coefficient than the swept-back wing.

In Fig. 9, the normal-force and pitching-moment coefficients are given as functions of the sweep-back angle for a fixed angle of attack and aspect ratio. One expects the effects of the wing-tip vortex system to decrease as the sweep-back angle increases, and this trend is shown by the present results. We note that the present calculations were made without considering the possibility of leading-edge separation.

B. Delta Wings

In Figs. 3 and 10, we illustrate the salient difference between the present method and that of Rehbach.[38] Beginning with a rectangular wing, he progressively shortens the leading edge until he obtains a delta wing. He solves the initial problem for the rectangular wing and each of the intermediate problems for the trapezoidal wings (he showed five in his paper). The number of elements is not reduced in this process. On the other hand, the present scheme employes a uniform-element lattice, which probably has substantially fewer elements than Rehbach's deformed lattice. Moreover, only the desired planform is considered; there are no intermediate problems. Consequently, the present scheme is expected to require substantially less computing time and storage than Rehbach's. Moreover, before deciding on the present arrangement, we attempted to deform a rectangular wing into a delta wing (a scheme similar to Rehbach's). We found that the shape of the wake often failed to converge, and when the shape did converge, the aerodynamic loads often failed to converge as the number of elements was increased. (We note that Rehbach only presented the results for one planform, one set of elements, and three angles of attack, and that his results do not agree as closely with the experimental data as the

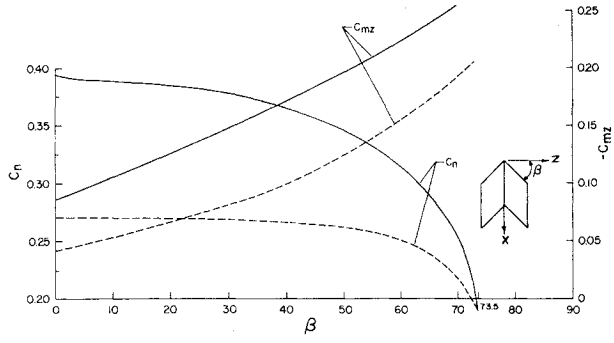

Fig. 9 Normal-force coefficient and pitching-moment coefficient vs sweep-back angle, $\mathcal{R}=1$, $\alpha=10°$. 6×6 lattice: ——— Linear; —— Nonlinear.

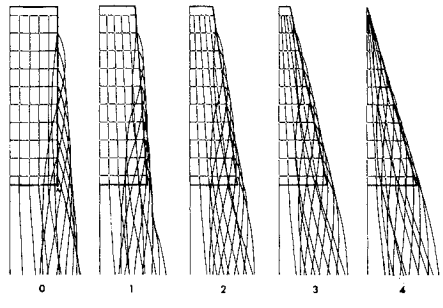

Fig. 10 Rehbach's progressive deformation of rectangular wing.

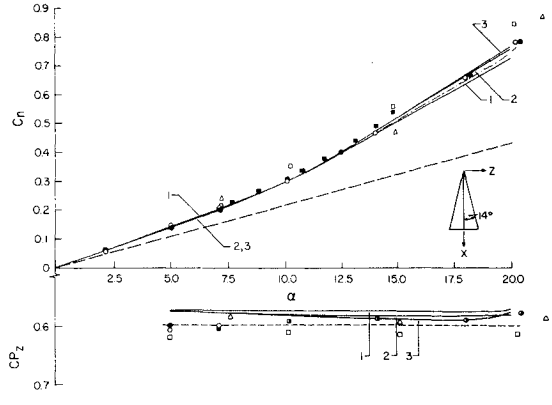

Fig. 11 Normal-force coefficient and position of center of pressure vs angle of attack, $\mathcal{R}=1$. Numerical results: —— Lawrence;[42] □ Sacks, et al.[24] —— Polhamus;[27] △ Rehbach;[38] ■ Mook and Maddox;[36] — Present Method. Curve No. 1: 4×4 lattice; curve No. 2: 5×5 lattice; curve No. 3: 6×6 lattice. Experimental results: • Bartlett and Vidal;[39] ○ Peckham.[3]

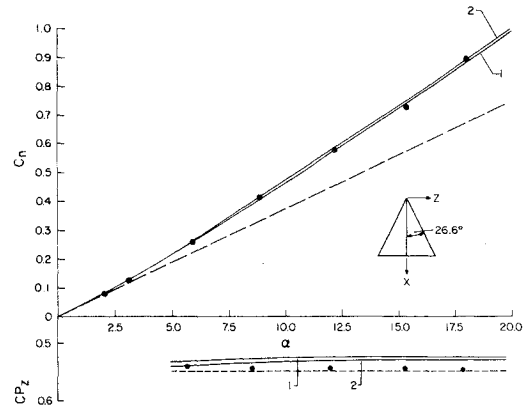

Fig. 12 Normal-force coefficient and position of center of pressure vs angle of attack, $\mathcal{R}=2$. Numerical results: —— Lawrence;[42] — Present method. Curve No. 1: 5×5 lattice; curve No. 2: 6×6 lattice. Experimental results: • Bartlett and Vidal.[39]

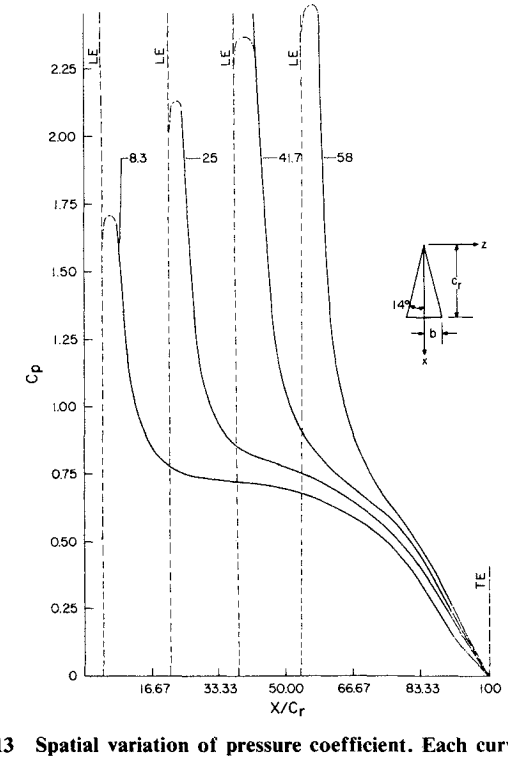

Fig. 13 Spatial variation of pressure coefficient. Each curve is for constant value of $(z/b)\times 100$, 6×6 lattice, $\mathcal{R}=1$, $\alpha=20°$. — Calculated; ——— Extrapolated.

present results.) Apparently, these problems are due to round-off errors resulting from the very close spacing of the grid of discrete singularities near the apex. The present scheme avoids this problem.

Figure 3 depicts an actual solution in which the positions of the finite segments in the wake were determined. The arrangement of the vortex line is shown in three views drawn to scale.

In Fig. 11, the normal-force coefficient and the position of the center of pressure are given as functions of the angle of attack, respectively. The graphs show the effect of increasing the number of elements and provide comparisons with other analytical, numerical, and experimental investigations. In Fig. 12, the same coefficients are given as functions of the angle of attack for delta wings having an aspect ratio of 2.

In Fig. 13, the spatial variation of the pressure coefficient is given for a delta wing having a unit aspect ratio. Each curve gives the chordwise variation at a fixed spanwise station. The dotted portions were faired in to make the pressure satisfy the known conditions along the edges. In all the numerical examples, the convergence requirements of Sec. IV were satisfied.

Numerical experiments indicate that the wake adjoining the trailing edge has only a slight effect on the results; hence, one can use only one or two finite segements in each vortex line of the wake adjoining the trailing edges. This can reduce the computation time substantially.

VI. Conclusions

The numerical examples indicate that the present method can be used to predict accurately the aerodynamic characteristics for wings having low aspect ratios at large angles of attack as long as the lines of separation are fixed at the sharp edges and vortex bursting does not occur. Adding wing-tip or leading-edge vortex systems to the model of the lifting-surface flowfield increases the predicted pressure difference over the entire wing; the greatest increase occurs in the regions near the lines of separation.

References

[1]Marsden, D. J., Simpson, R. W., and Rainbird, B. E., "An Investigation into the Flow over Delta Wings at Low Speeds with Leading Edge Separation," Rept. 114, Feb. 1958, College of Aeronautics, Cranfield, England.

[2]Peckham, D. H., "Low-Speed Wind-Tunnel Tests on a Series of Uncambered Slender, Pointed Wings with Sharp Edges," ARC R&M 2834, Aeronautical Research Council, London.

[3]Bergesen, A. J. and Porter, J. D., "An Investigation of the Flow Around Slender Delta Wings with Leading-Edge Separation," Rept. 510, May 1960, Princeton University, Princeton, N. J.

[4]Hummel, D., "Study of the Flow around Sharp-Edged Slender Delta Wings with Large Angles of Attack," NASA TT F-15, 107, Sept. 1973 (Translation of *Zeitschrift für Flugwissenschaften*, Vol. 15, Oct. 1967, pp. 376-385).

[5]Winter, H., "Flow Phenomena on Plates and Airfoils of Short Span," Rept. 798, 1937, NACA.

[6]Scholz, von N., "Kraft und Druckverteilungsmessungen an Tragflächen Kleiner Streckung," *Forscharb. Ing. Wes.*, No. 16, 1949, pp. 85-92.

[7]Ermolenko, S. D., "Nonlinear Theory of Small Aspect Ratio Wings," *Soviet Aeronautics* (in English), Vol. 9, pp. 5-11, March 1966.

[8]Belotserkovskiy, S. M., "Calculation of the Flow around Wings of Arbitrary Planforms in a Wide Range of Angles of Attack," TT F-12, 291, May 1969, NASA.

[9]Lamar, J. E., "Extension of Leading-Edge-Section Analogy to Wings with Separated Flow around the Side Edges at Subsonic Speeds," TR R-428, 1974, NASA.

[10]Wentz, W. H. and Kohlman, D. L., "Vortex Breakdown on Slender Sharp-Edged Wings," *Journal of Aircraft*, Vol. 8, March 1971, pp. 156-161.

[11]Sutton, E. P., "Some Observations of the Flow over a Delta-Winged Model with 55-deg Leading-Edge Sweep, at Mach Numbers between 0.4 and 1.8," ARC R&M 3190, Nov. 1955, Aeronautical Research Council, London.

[12]Squire, L. C., Jones, J. G., and Stanbrook, A., "An Experimental Investigation of the Characteristics of Some Plane and Cambered 65° Delta Wings at Mach Numbers from 0.7 to 2.0," ARC R&M 3305, July 1961, Aeronautical Research Council, London.

[13]Bateman, J. E. B. and Hanes, A. B., "A Comparison of Results in the A. R. A. Transonic Tunnel on a Small and a Large Model of a Slender Wing," R&M 3287, Sept. 1961, Aeronautical Research Council, London.

[14]Dee, F. W. and Nicholas, O. P., "Flight Determination of Wing-Flow Patterns and Buffet Boundaries for the Fairey Delta 2 Aircraft at Mach Numbers between 0.4 and 1.3, and Comparison with Wind-Tunnel Results," R&M 3482, Sept. 1964, Aeronautical Research Council, London.

[15]Stahl. W., Hartmann, K., and Schneider, W., "Force and Pressure Measurements on Slender Delta Wing at Transonic Speeds and Varying Reynolds Numbers," Rept. 71A01, June 1971, Aerodynamische Versuchsanstalt Göttingen.

[16]Wentz, W. H., "Effects of Leading-Edge Camber on Low-Speed Characteristics of Slender Delta Wings," CR-2002, 1972, NASA.

[17]Bollay, W., "A Theory for Rectangular Wings of Small Aspect Ratio," *Journal of the Aeronautical Sciences*, Vol. 4, Jan. 1937, pp. 294-296.

[18]Gersten, K., "Calculation of Nonlinear Aerodynamic Stability Derivatives of Aeroplanes," AGARD Rep. 342, April 1961.

[19]Garner, H. C. and Lehrian, "Nonlinear Theory of Steady Forces on Wings with Leading-Edge Flow Separation," R&M 3375, Feb. 1963, Aeronautical Research Council, London.

[20]Legendre, R., "E'coulement du Voisinage de la Pointe Avante d'une dile a Forte Flache dux Incidences Moyennes," *La Recherche Aeronautique*, No. 31, 1953.

[21]Brown, C. E. and Michael, W. H., "Effect of Leading Edge Separation on the Lift of a Delta Wing," *Journal of Aeronautical Sciences*, Vol. 21, Oct. 1954, pp. 690-694.

[22]Mangler, K. W. and Smith, J. H. B., "Calculation of the Flow Past Slender Delta Wings with Leading Edge Separation," RAE Rept. 2593, May 1957, Royal Aircraft Establishment, Farnsborough, England.

[23]Smith, J. H. B., "Improved Calculations of Leading-Edge Separation from Slender Delta Wings," RAE Tech Rept. 66070, March 1965, Royal Aircraft Establishment, Farnsborough, England.

[24]Sacks, A. H., Lundberg, R. E., and Hanson, C. W., "A Theoretical Investigation of the Aerodynamics of Slender Wing-Body Combinations Exhibiting Leading-Edge Separation," CR-719, 1967, NASA.

[25]Nagia, R. K. and Hancock, G. J., "Delta Wings with Longitudinal Camber at Low Speed," CP 1129, 1970, Aeronautical Research Council, London.

[26]Polhamus, E. C., "A Concept of the Vortex Lift of Sharp-Edge Delta Wings Based on a Leading-Edge Suction Analogy," TN D-3767, 1966, NASA.

[27]Polhamus, E. C., "Predictions of Vortex-Lift Characteristics by a Leading-Edge-Suction Analogy," *Journal of Aircraft*, Vol. 8, April 1971, pp. 193-199.

[28]Bradley, R. G., Smith, C. W., and Bhateley, I. C., "Vortex-Lift Prediction for Complex Wing Planforms," *Journal of Aircraft*, Vol. 10, June 1973, pp. 379-381.

[29]Earnshaw, P. B., "An Experimental Investigation of the Structure of a Leading-Edge Vortex," R&M 3281, March 1961, Aeronautical Research Council, London.

[30]James, R. M., "On the Remarkable Accuracy of the Vortex Lattice Discretization in Thin-Wing Theory," Rept. DAC-67211, 1969, McDonnell Douglas Aircraft Co., Long Beach, Calif.

[31]Hough, G. R., "Remarks on Vortex-Lattice Methods," *Journal of Aircraft*, Vol. 10, May 1973, pp. 314-317.

[32]Rubbert, P. E., "Theoretical Characteristics of Arbitrary Wings by a Nonplanar Vortex Lattice Method," Rept. D6-9244, 1962, Boeing Co., Seattle, Wash.

[33]Hedman, S. G., "Vortex Lattice Method for Calculation of Quasi-Steady-State Loadings on Thin Elastic Wings," Rept. 105, 1966, Aeronautical Research Inst. of Sweden, Stockholm, 1966.

[34]Belotserkovskiy, S. M., *Theory of Thin Wings in Subsonic Flow*, (translated from Russian), Plenum Press, New York, 1967, pp. 112-118.

[35]Kalman, T. P., Rodden, W. P., and Giesing, J. P., "Aerodynamic Influence Coefficients by the Doublet Lattice Method for Interfering Nonplanar Lifting Surfaces Oscillating in a Subsonic Flow (Pt I)," Rept. DAC-67977, 1967, McDonnell Douglas Corp., Long Beach, Calif.

[36]Mook, D. T. and Maddox, S. A., "Extension of a Vortex-Lattice Method to Include the Effects of Leading-Edge Separation," *Journal of Aircraft*, Vol. 11, Feb. 1974, pp. 127-128.

[37]Rehbach, C., "Calculation of Flows around Zero-Thickness Wings with Evalute Vortex Sheets," TT F-15, 183, 1973, NASA.

[38]Rehbach, C., "Numerical Investigation of Vortex Sheets Issuing from Separation Line near the Leading Edge," TT F-15, 530, 1974, NASA.

[39]Bartlett, G. E. and Vidal, R. J., "Experimental Investigation of Influence of Edge Shape on the Aerodynamic Characteristics of Low-Aspect-Ratio Wings at Low Speeds," *Journal of the Aeronautical Sciences*, Vol. 22, Aug. 1955, pp. 517-533.

[40]Kirkpatrick, D. L. I., "Investigation of the Normal Force Characteristics of Slender Delta Wings with Various Rhombic Cross Sections in Subsonic Conical Flow," CP 922, Dec. 1965, Aeronautical Research Council, London.

[41]Kandil, O. A., "Prediction of the Steady Aerodynamic Loads on Lifting Surfaces Having Sharp-Edge Separation," Ph. D. Dissertation, Engineering Science and Mechanics Dept., Virginia Polytechnic Inst. and State Univ., Dec. 1974.

[42]Lawrence, H., "The Lift Distribution on Low-Aspect-Ratio Wings at Subsonic Speeds," *Journal of the Aeronautical Sciences*, Vol. 18, Oct. 1951, pp. 683-695.